VIP Phototherapeutic Agents

DOI: 10.1002/anie.200902837

Photoactive Hybrid Nanomaterial for Targeting, Labeling, and Killing Antibiotic-Resistant Bacteria**

Cristian A. Strassert, Matthias Otter, Rodrigo Q. Albuquerque, Andrea Höne, Yolanda Vida, Berenike Maier, and Luisa De Cola**

Phototherapeutic agents constitute a powerful armory for treating cancers and infectious diseases,[1–3] and nanotechnology has produced multifunctional arrays with targeted cytotoxicity and labeling capabilities.[4–6] Such structures must be robust, well-characterized, and able to be produced at industrial scale.[7] Herein we show a multifunctional hybrid material based on zeolite L able to target, label, and photoinactivate pathogenic and antibiotic-resistant bacteria. A highly green-luminescent dye was inserted into the channels of zeolite L nanocrystals for imaging and to label the cells. The outer surface was functionalized with a photosensitizer that forms toxic singlet oxygen upon red-light irradiation and with amino groups for targeting the living microorganisms. The resulting trifunctional nanomaterial therefore shows intense green fluorescence and efficient $^1O_2$ photoproduction. As a consequence, it can target, label, and photoinactivate antibiotic-resistant *Escherichia coli* and *Neisseria gonorrhoeae*. These results open fascinating possibilities for the development of the next generation of photosensitizers for phototherapy.

Recent challenges of modern pharmacology include resistance of bacteria to multiple antibiotics and of neoplastic cells to chemotherapeutics, which on the other hand cause undesired side effects. Photodynamic therapy (PDT) is an established cancer and macular degeneration treatment[1,2] and constitutes an alternative against antibiotic-resistant bacteria.[3] In PDT, a photosensitizer generates cytotoxic $^1O_2$ upon irradiation with light. The ultimate goal is to develop one single structure possessing targeted therapeutic agents, efficient $^1O_2$ photoproduction, and imaging capacities.[1–3]

Nanoparticles have been investigated as therapeutic, sensing, and imaging agents, relying on surface modification with biocompatible moieties.[8–13] Also, it has been recently reported that amino-modified zeolite L microcrystals are able to bind to the surface of *E. coli* cells.[14] Zeolite L is an aluminosilicate possessing channels able to host a variety of dyes[15] and constitutes a nontoxic nanocarrier that can be functionalized on its surface and orthogonally modified on the channel entrances.[16] No attempt has been made to date to exploit these properties for therapeutic purposes. Phthalocyanines are excellent for the development of phototherapeutic agents owing to their low toxicity, high stability, efficient $^1O_2$ generation, and intense light absorption in the therapeutic window.[1–3,17] In particular, zinc(II) and silicon(IV) phthalocyaninates have been investigated as promising photosensitizers.[1–3] Amino groups are also important to modulate the biological activity of these dyes,[18,19] which can be conjugated to a variety of structures with interesting photophysical and photobiological properties.[20–24] However, aggregation is a drawback that must be avoided in order to exploit the photosensitizing ability of these macrocycles.[17]

We designed a nanoarchitecture to provide fluorescence labeling, photosensitizing activity, and cellular adhesion (Figure 1). We used zeolite L nanocrystals, 50 nm in both length and diameter, loaded with the green emitter DXP (*N*,*N*′-bis(2,6-dimethylphenyl)perylene-3,4,9,10-tetracarbodiimide), which was encapsulated by gas-phase insertion.[15] The DXP-loaded zeolite L nanocrystals were further functionalized with tetra-*tert*-butyl-substituted Si^{IV} phthalocyanine dihydroxide (PC) by axial attachment of the macrocycle's central silicon atom to OH groups of the zeolite L surface. Therefore, PC can be regarded as an extension of the structure of zeolite L (Figure 1). Aggregation of the macrocycle is avoided by axial binding of the central Si^{IV} atom to the surface and by steric repulsion between the *tert*-butyl groups. Finally, the surface of the multifunctional zeolites was coated with amino groups to promote the adhesion to bacteria.[14]

The DXP loading was kept below 1% to avoid the formation of J aggregates inside the zeolite L channels, which are known to lower the photoluminescence quantum yield and to cause a bathochromic shift of the emitted wavelength.[25] Such low concentrations give rise to uniform green luminescence. Using fluorescence spectroscopy, we estimated a coverage of 17×10^3 PC molecules per crystal. In this calculation, the zeolites were approximated as having a cylindrical shape with height and diameter of 50 nm. This approach underestimates the effective surface area of the

[*] Dr. C. A. Strassert, Dipl.-Chem. M. Otter, Dr. R. Q. Albuquerque, Dr. Y. Vida, Prof. L. De Cola
Physikalisches Institut and Center for Nanotechnology (CeNTech)
Westfälische Wilhelms-Universität Münster
Heisenbergstrasse 11, 48149 Münster (Germany)
Fax: (+49) 251-980-2834
E-mail: ca.s@uni-muenster.de
decola@uni-muenster.de
Homepage: http://www.uni-muenster.de/Physik.PI/DeCola/
Dipl.-Biol. A. Höne, Prof. B. Maier
Institut für Allgemeine Zoologie und Genetik
Westfälische Wilhelms-Universität Münster (Germany)

[**] We thank Prof. Peters for the *E. coli* samples and S. Fibikar for helping us with the acquisition of the SEM images. We also thank the DFG (grant number GZ: INST 211/418-1 FUGG) for financial support provided for the acquisition of the time-resolved confocal microscope. This work was also supported by the DFG (A.H. and B.M.: SFB629), the Alexander von Humboldt Foundation (R.Q.A.), and Fundación Ramón Areces (Y.V.).

Supporting information for this article, including experimental details, is available on the WWW under http://dx.doi.org/10.1002/anie.200902837.

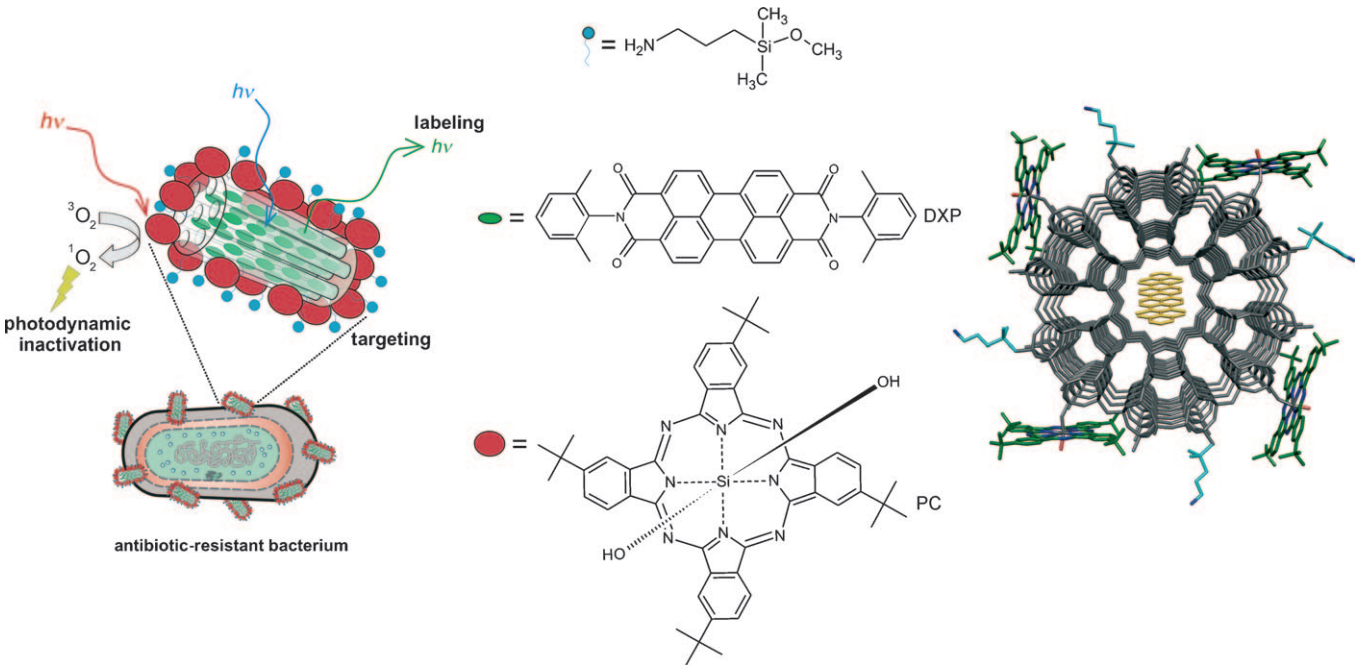

Figure 1. Pictorial view of the multifunctional nanomaterial used to target, label, and photoinactivate antibiotic-resistant bacteria. The zeolite L nanocrystal is loaded with the DXP emitter (green ellipsoid), and its surface is functionalized with a phthalocyanine derivative (red ellipsoid) and with amino groups (blue circles), where the latter provide noncovalent binding of the hybrid nanomaterial to the bacterial surface. On the right, a schematic view of the connection of the functional groups to the zeolite L framework is shown.

single crystals, which are irregular and exhibit terraces. The area of a single PC molecule can be estimated as 2 nm^2, meaning that 6×10^3 molecules could be attached to an idealized cylindrical nanocrystal of zeolite L (surface area ca. 12000 nm^2). This value is smaller than that experimentally obtained for the nanomaterial but is of the same order of magnitude and indicates that the effective surface area of the nanocrystals is larger. This result suggests that most of the crystals' surface is covered with PC, which contributes to the photobiological efficiency (see below).

The photophysical properties are shown in Figure 2, which depicts excitation and emission spectra of the hybrid system and fluorescence microscopy images. Figure 2a shows the characteristic emission and excitation spectra of DXP.[26] The green fluorescence exhibited by the sample upon excitation of DXP is shown on the right. Figure 2b shows the distinctive excitation and emission spectra of PC,[20,21] together with a microscopy image of its red luminescence, which demonstrates that the zeolite L surface hinders the formation of aggregates. We performed an additional experiment with 4 μm long zeolite L crystals, showing that upon excitation of PC, a bright red luminescence is only observed on the functionalized zeolite L crystals. The unbound PC remains aggregated in the form of nonfluorescent green crystals (Figure S1 in the Supporting Information).

When monitoring the emission of PC (Figure 2b), the excitation spectrum only shows the Soret and Q bands of the macrocycle (no DXP absorption band is detected). No electronic energy transfer occurs from DXP to PC, which is a consequence of the electronic decoupling between the chromophores localized inside the zeolite L channels and those attached to the surface.[15,16] Both dyes constitute independent photophysical labels that can be separately detected and addressed, thus allowing the use of DXP as an internal standard to monitor the labeling of the bacteria.

Figure 2c shows that upon excitation of PC at 670 nm an intense emission with maximum at 1275 nm is obtained, which matches the characteristic phosphorescence of $^1O_2$.[20,21] The corresponding excitation spectrum was recorded by monitoring the emission at 1275 nm, and it reproduces the Soret and Q bands of the macrocycle (compare with Figure 2b), which confirms that only PC in the monomeric form is responsible for the $^1O_2$ generation. The $^1O_2$ quencher DABCO (1,4-diazabicyclo[2.2.2]octane) completely suppressed the emission at 1275 nm. No $^1O_2$ photoproduction was observed when the nanocrystals were not functionalized with PC.

A strain of *E. coli* bacteria resistant to chloramphenicol was employed as a model biological target. Gram-negative bacteria are harder to photoinactivate owing to the presence of an additional outer membrane including a lipopolysaccharide, which renders them more resistant to common photosensitizing drugs.[3] The amino-functionalized hybrid nanomaterial labeled the *E. coli* cells, as can be seen in the microscopy images (Figure 3a,b and Figure S2 in the Supporting Information). The SEM pictures of labeled *E. coli* bacteria (Figure 3c and inset) confirm the adhesion of the hybrid nanomaterial. The amino groups provide an effective anchor to the bacterial surface owing to their capacity for hydrogen bonding and electrostatic bonding. The zeta potential measurements (Table S1 in the Supporting Information) demonstrate that the amino-functionalized zeolites are positively charged, favoring adhesion to the negatively charged

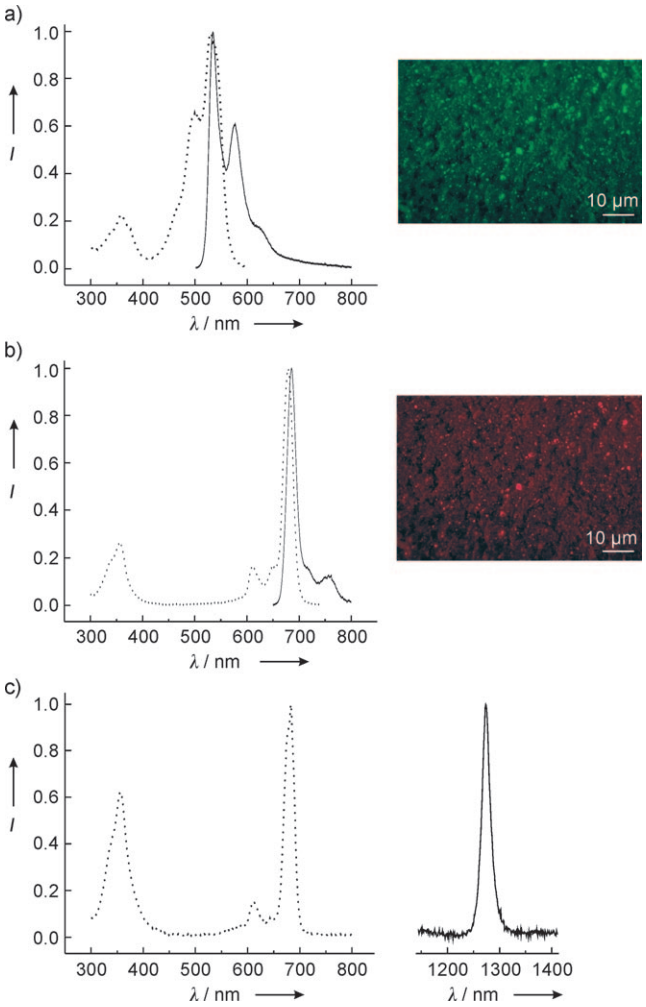

Figure 2. Excitation (dotted line) and emission (solid line) spectra of DXP (a; $\lambda_{em} = 620$ nm, $\lambda_{exc} = 480$ nm), PC (b; $\lambda_{em} = 750$ nm, $\lambda_{exc} = 630$ nm), and PC and $^1O_2$ (c; $\lambda_{em} = 1275$ nm, $\lambda_{exc} = 670$ nm) in a suspension of the nanomaterial in CH_2Cl_2 (a,b) or CD_2Cl_2 (c). Fluorescence microscopy images were acquired by exciting at 420–490 nm (a) or at 575–630 nm (b).

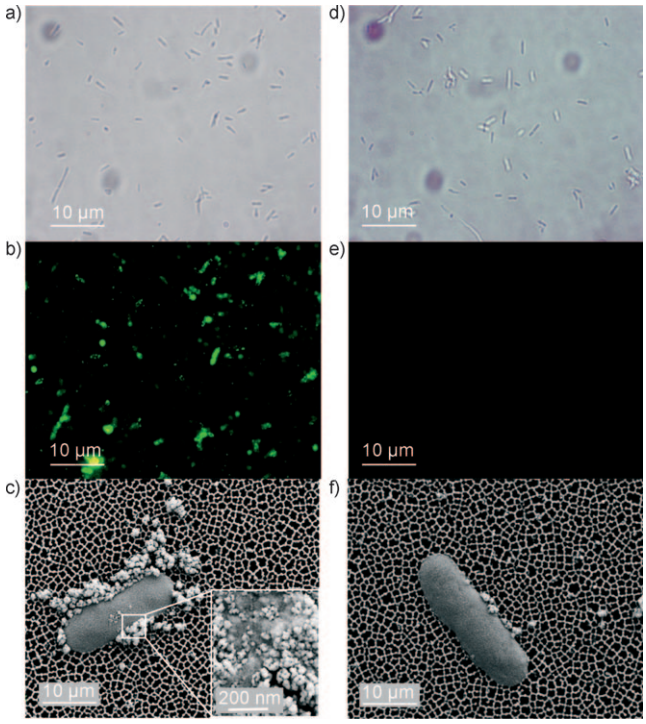

Figure 3. Interaction of the hybrid nanomaterials with *E. coli* cells in phosphate-buffered saline solution (PBS). a) Bright-field microscopy, b) fluorescence microscopy ($\lambda_{exc} = 470$–490 nm), and c) SEM images of bacteria treated with the amino-functionalized nanomaterial. The inset in (c) shows a magnified portion of the bacterium showing the adhesion of the nanomaterial to the cell surface. d) Bright-field microscopy, e) fluorescence microscopy ($\lambda_{exc} = 470$–490 nm), and f) SEM images of bacteria treated with the nanomaterial without amino functionalization. Comparison of the left with the right part of the figure shows the targeting effect of the amino groups (see text for details).

membranes of the bacteria. Zeolites without amino groups, in contrast, display a negative zeta potential. No cell adhesion can therefore occur between the negatively charged surface of the bacteria and the zeolites without amino groups. This conclusion is confirmed by fluorescence microscopy and SEM analysis (Figure 3e, f).

To explore the photobiological activity, a photodynamic treatment was carried out by suspending *E. coli* cells with the hybrid nanomaterial and irradiating the sample for 2.5 h in the wavelength range between 570 and 900 nm (irradiance of 3 mW cm^{-2}). In this spectral region only the PC is excited to produce $^1O_2$, thus avoiding photobleaching of the DXP entrapped inside the zeolite channels. Every 30 min samples were stained with propidium iodide (PI), a cationic dye that selectively penetrates the membrane of dead cells, which is possible owing to their altered membrane potential, and exhibits strong red emission upon intercalation into DNA.[27] This method allows the visualization of inactivated bacteria. Figure 4a shows a time sequence of fluorescence pictures of *E. coli* cells labeled with the hybrid nanomaterial, taken during the photodynamic treatment. The progressing cell death can be monitored by the color change: the living cells exhibit green emission from DXP labeling, and the inactivated ones show the red fluorescence from the PI.

Quantification of the dead bacteria as a function of irradiation time is shown in Figure 4b, obtained by analysis of the bright-field and fluorescence microscopy images acquired during the photodynamic treatment. Only concomitant irradiation and PC functionalization led to the successful photoinactivation of the cells, thus confirming the photodynamic effect. No significant cell death was detected in the absence of PC or of irradiation. The photodynamic inactivation was complete (95%) after 2 h, corresponding to a light dose of 27 J cm^{-2}, which is smaller than other values described in the literature.[28] Similar results were obtained with a pathogenic strain of tetracycline-resistant *N. gonorrhoeae*, where the inactivation efficiency was 95% (Figure 4c).

In conclusion, we developed an innovative potential phototherapeutic tool by using a multifunctional nanoarchitecture constructed on the zeolite L platform. The robust assembly is easy to synthesize by combining industry-standard chromophores and a well-defined solid substrate. We dem-

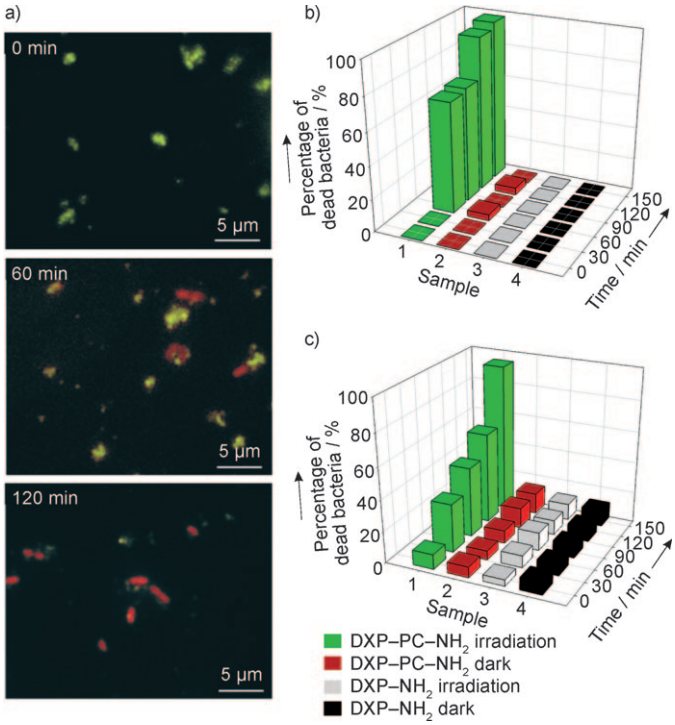

Figure 4. a) Time-lapse fluorescence microscopy images of the chloramphenicol-resistant *E. coli* cells during photodynamic treatment in PBS, recorded with excitation in the range 470–490 nm. The green emission comes from the DXP-filled hybrid nanomaterial, while the red one arises from the PI–DNA complex, which is only formed inside dead bacteria. b) Percentage of inactivated *E. Coli* and c) *N. gonorrhoeae* cells as a function of time and experimental conditions.

onstrated that the hybrid nanomaterial efficiently produces singlet oxygen and adheres to bacterial surfaces, leading to targeting, labeling, and photoinactivation capabilities against antibiotic-resistant bacteria. These results open fascinating possibilities for the photodynamic treatment of infectious and neoplastic diseases, shining new light onto the design of third-generation photosensitizers for PDT.

Received: May 27, 2009
Published online: September 3, 2009

Keywords: antibiotic-resistant bacteria · drug design · fluorescence · phthalocyanines · singlet oxygen

[1] T. J. Dougherty, C. J. Gomer, B. W. Henderson, G. Jori, D. Kessel, M. Korbelik, J. Moan, Q. Peng, *J. Natl. Cancer Inst.* **1998**, *90*, 889–905.
[2] A. Juzeniene, Q. Peng, J. Mohan, *Photochem. Photobiol. Sci.* **2007**, *6*, 1234–1245.
[3] M. R. Hamblin, T. Hasan, *Photochem. Photobiol. Sci.* **2004**, *3*, 436–450.
[4] M.-R. Choi, K. J. Stanton-Maxey, J. K. Stanley, J. C. S. Levin, R. Bardhan, D. Akin, S. Badve, J. Sturgis, J. P. Robinson, R. Bashir, N. J. Halas, S. E. Clare, *Nano Lett.* **2007**, *7*, 3759–3765.
[5] M. Ferrari, *Nat. Rev. Cancer* **2005**, *5*, 161–171.
[6] G. M. Whitesides, *Small* **2005**, *1*, 172–179.
[7] M. Eaton, *Nat. Mater.* **2007**, *6*, 251–253.
[8] A. Burns, H. Ow, U. Wiesner, *Chem. Soc. Rev.* **2006**, *35*, 1028–1042.
[9] R. C. Somers, M. G. Bawendi, D. G. Nocera, *Chem. Soc. Rev.* **2007**, *36*, 579–591.
[10] L. Tetard, A. Passian, K. T. Venmar, R. M. Lynch, B. H. Voy, G. Shekhawat, V. P. Dravid, T. Thundat, *Nat. Nanotechnol.* **2008**, *3*, 501–505.
[11] T. Rajh, *Nat. Mater.* **2006**, *5*, 347–348.
[12] W. Jiang, B. Y. S. Kim, J. T. Rutka, W. C. W. Chan, *Nat. Nanotechnol.* **2008**, *3*, 145–150.
[13] E. Tasciotti, X. W. Liu, R. Bhavane, K. Plant, A. D. Leonard, B. K. Price, M. M. C. Cheng, P. Decuzzi, J. M. Tour, F. Robertson, M. E. Ferrari, *Nat. Nanotechnol.* **2008**, *3*, 151–157.
[14] Z. Popovic, M. Otter, G. Calzaferri, L. De Cola, *Angew. Chem.* **2007**, *119*, 6301–6304; *Angew. Chem. Int. Ed.* **2007**, *46*, 6188–6191.
[15] G. Calzaferri, S. Huber, H. Maas, C. Minkowski, *Angew. Chem.* **2003**, *115*, 3860–3888; *Angew. Chem. Int. Ed.* **2003**, *42*, 3732–3758.
[16] M. Busby, H. Kerschbaumer, G. Calzaferri, L. De Cola, *Adv. Mater.* **2008**, *20*, 1614–1618.
[17] C. A. Strassert, G. M. Bilmes, J. Awruch, L. E. Dicelio, *Photochem. Photobiol. Sci.* **2008**, *7*, 738–747.
[18] N. B. Rumie Vittar, C. G. Prucca, C. A. Strassert, J. Awruch, V. A. Rivarola, *Int. J. Biochem. Cell Biol.* **2008**, *40*, 2195–2205.
[19] N. L. Oleinick, A. R. Antunez, M. E. Clay, B. D. Rihter, M. E. Kenney, *Photochem. Photobiol.* **1993**, *57*, 242–247.
[20] K. Ishii, M. Shiine, Y. Kikukawa, N. Kobayashi, T. Shiragami, J. Matsumoto, M. Yasuda, H. Suzuki, H. Yokoi, *Chem. Phys. Lett.* **2007**, *448*, 264–267.
[21] K. Ishii, Y. Kikukawa, M. Shiine, N. Kobayashi, T. Tsuru, Y. Sakai, A. Sakoda, *Eur. J. Inorg. Chem.* **2008**, 2975–2981.
[22] S. Dayal, C. Burda, *J. Am. Chem. Soc.* **2008**, *130*, 2890–2891.
[23] N. Nishiyama, A. Iriyama, W.-D. Jang, K. Miyata, K. Itaka, Y. Inoue, H. Takahashi, Y. Yanagi, Y. Tamaki, H. Koyama, K. Kataoka, *Nat. Mater.* **2005**, *4*, 934–941.
[24] M. E. Wieder, D. C. Hone, M. J. Cook, M. M. Handsley, J. Gavrilovic, D. A. Russell, *Photochem. Photobiol. Sci.* **2006**, *5*, 727–734.
[25] M. Busby, C. Blum, M. Tibben, S. Fibikar, G. Calzaferri, V. Subramaniam, L. De Cola, *J. Am. Chem. Soc.* **2008**, *130*, 10970–10976.
[26] G. Calzaferri, K. Lutkouskaya, *Photochem. Photobiol. Sci.* **2008**, *7*, 887–918.
[27] G. Nebe-von-Caron, P. J. Stephens, C. J. Hewitt, J. R. Powell, R. A. Badley, *J. Microbiol. Methods* **2000**, *42*, 97–114.
[28] V. Mantareva, V. Kussovski, I. Angelov, E. Borisova, L. Avramov, G. Schnurpfeil, D. Wöhrle, *Bioorg. Med. Chem.* **2007**, *15*, 4829–4835.

